Catalysis Science & Technology

PAPER

View Article Online
View Journal



# Toward a mechanistic understanding of oxidative homocoupling: the Glaser–Hay reaction†

Cite this: DOI: 10.1039/c4cy00322e

Jesús Jover,[a] Philipp Spuhler,[b] Ligang Zhao,[b] Ciarán McArdle[b] and Feliu Maseras*[ac]

Received 13th March 2014,
Accepted 15th May 2014

DOI: 10.1039/c4cy00322e

www.rsc.org/catalysis

The copper-catalyzed oxidative homocoupling of terminal alkynes has been studied with DFT methods. The role of Cu(I) or Cu(II) as the initial oxidation state as well as the effect of the changes in the substrate and the base have been examined. Oxidants responsible for outer- and inner-sphere electron transfer processes have also been investigated. The Cu/$O_2$ interactions, which arise when dioxygen is employed as the oxidant, have been studied explicitly to fully describe the 4-electron reduction process, providing a plausible mechanism that could serve as a model for other aerobic oxidative couplings. The obtained results completely agree with the reported experimental data: the computed free energy barriers are low enough for the reactions to proceed at room temperature, and electron-poor alkynes and stronger bases lead to faster reactions.

## Introduction

Metal-mediated coupling reactions have become one of the main groups of tools to carry out the formation of C–C bonds.[1] The importance of cross-coupling between R–X (X = halide) and R′–Y (Y = electropositive group) was recognized by the Nobel Prize in 2010.[2] Not all systems are however amenable to cross-coupling, and as a result, homocoupling, where the reaction occurs between two identical molecules, is also a subject of interest. In homocoupling, an external reducing or oxidizing[3] agent is often necessary to bring the metal back to its initial oxidation state. The use of dioxygen in oxidative homocoupling is particularly appealing because only water is formed as the byproduct of oxidation.[4]

One of the earliest and most simple examples of oxidative homocoupling is the Glaser reaction, reported originally in 1869.[5] Glaser observed that a mixture of phenylacetylene, copper(I) chloride and ammonium hydroxide in ethanol, when exposed to air, smoothly formed diphenyldiacetylene (Scheme 1). The scope of the reaction was later expanded, as it was revealed that $O_2$ can be replaced by many other oxidants.[6,7] A crucial modification of the reaction, reported by Hay in the 1960s,[8] indicated that addition of nitrogen ligands such as TMEDA (*N*,*N*,*N*′,*N*′-tetramethylethylenediamine) allowed the reaction to be carried out under mild conditions using copper(I) chloride as the catalyst. Since then a variety of copper(I) and (II) salts and nitrogen ligands, *i.e.* tertiary amines or pyridines, have been used to perform oxidative coupling of acetylenes providing good results.[9–12] In most experiments, a ligand excess or an external base is added because it has been demonstrated that the reaction is faster under basic conditions. Different bases ranging from ammonium hydroxide employed by Glaser to organic amines[11–13] (*e.g.* piperidine, $NEt_3$, *etc.*) or inorganic salts such as sodium carbonate or acetate have been employed.[14,15] Another piece of relevant experimental information states that acidic acetylenes produce the fastest reaction rates,[16] indicating that terminal proton abstraction plays a crucial role on the mechanism.

The Glaser–Hay reaction is technologically relevant, as the 1,3-diyne products obtained have a wide range of interesting applications in optical materials, organic conductors and molecular devices[17] as well as antifungal activity,[18] conducting polymers and liquid crystals.[19] On the other hand, the study of simple Glaser coupling reactions can serve as a benchmark for other, more complicated, oxidative coupling reactions where dioxygen is employed as the oxidant. Even more, improving our knowledge of these reactions can be used to better understand more complicated systems such as copper oxidases[20] and oxygenases[21] *e.g.* superoxide dismutase or tyrosinase, or even oxygen evolution systems.[22]

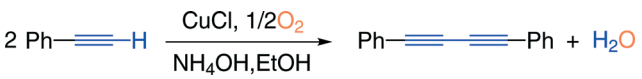


**Scheme 1** Oxidative coupling of phenylacetylene as described by Glaser.

[a] *Institute of Chemical Research of Catalonia (ICIQ), Avgda. Països Catalans 16, 43007 Tarragona, Catalonia, Spain. E-mail: fmaseras@iciq.es; Fax: (+34) 977920231*
[b] *Henkel AG & Co. KGaA, Henkelstrasse 67, 40589 Düsseldorf, Germany*
[c] *Departament de Química, Universitat Autònoma de Barcelona, 08193, Barcelona, Spain*

† Electronic supplementary information (ESI) available: Includes all computed potential energies, enthalpies, free energies, dispersion corrections, energy profiles and optimized structures, along the alternative Glaser–Hay pathways. See DOI: 10.1039/c4cy00322e

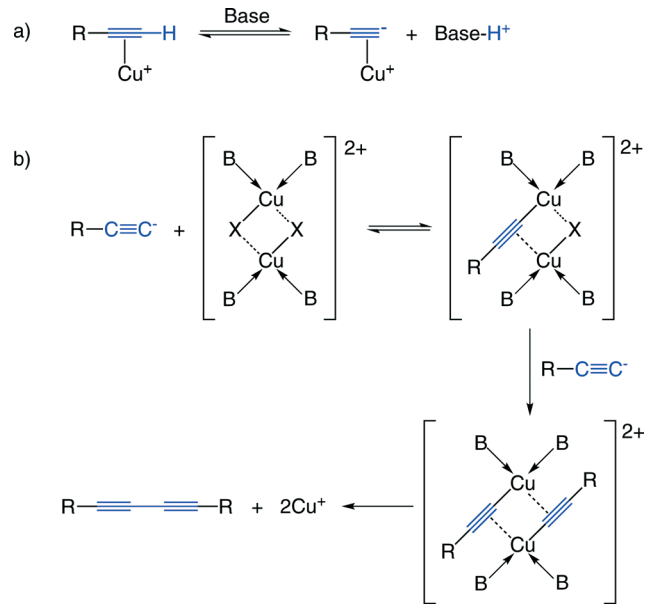


**Scheme 2** Bohlmann proposal for Glaser coupling of acetylenes (B = N ligand).

The detailed mechanism for the Glaser–Hay reaction remains to be determined. One of the most elaborate proposals was made by Bohlmann and co-workers in 1964,[16] summarized in Scheme 2. Based on their scheme, the reaction starts with the π-coordination of the triple bond to a copper(I) species that facilitates the activation of the terminal C–H bond by an external base. It was also proposed that a 1,3-diyne is formed by reductive elimination from a dinuclear copper(II) acetylide species (Scheme 2b). The Bohlmann mechanism neglects however the crucial oxidation step required to close the cycle, as part b) starts with copper(II) but ends up with copper(I).

An alternative mechanism was proposed more recently based on B3LYP DFT calculations.[23] A lot of emphasis was placed in this case in the interaction between copper and dioxygen, but the results had serious shortcomings. A detailed analysis of the computed thermodynamics reveals that although the reported potential energy barrier for the catalytic cycle is around 22 kcal $mol^{-1}$, the value increases above 50 kcal $mol^{-1}$ when free energy corrections are introduced. In addition, the proposed mechanism is completely specific for the employed reactants and it cannot explain why the reaction proceeds with different copper sources and oxidants. The suitability of the B3LYP functional for the characterization of $Cu_2O_2$ cores has also been called into question.[24,25] Some critical aspects of the reaction remain insufficiently explained in these proposals. In particular, a full mechanism must explain why the reaction seems to operate similarly regardless of the oxidant used. This is particularly shocking because of the use of one-electron oxidants, such as $K_3[Fe(CN)_6]$, and two- or four-electron oxidants, such as dioxygen. The mechanism must also explain why the reaction is faster under basic conditions[10–14] and when acidic acetylenes are used.[16] The role of dioxygen is particularly intriguing, since despite increased interest in the use of this oxidant in systems involving copper, little is known about its detailed reaction mechanism.[12,15,25–29] Computational studies of the role of copper/oxygen systems in homogeneous catalysis are scarce and focused on very specific cases.[23,30]

We present in this article a computational study on the mechanism for the Glaser–Hay reaction. Computational applications to aerobic oxidative coupling have been limited,[23] but they have a long story of success in cross-coupling[31] and other processes involving electron transfer in copper complexes.[32] As a first approach, a general mechanism valid for most outer sphere oxidants along with copper(I) reagents will be studied. At this stage $K_3[Fe(CN)_6]$ will be employed as the benchmark oxidant, representative of those that can be found in the literature. Then, the mechanism for the catalytic reaction starting from copper(II) will be evaluated with the same kind of oxidants. Afterwards, the full Glaser–Hay reaction mechanism will be studied to model the explicit interaction between the metal species and $O_2$ when the latter is used as the oxidant; this will show how dioxygen works in aerobic oxidative coupling copper-catalyzed reactions.

## Computational methods

All of the structures have been fully optimized in acetone using the Gaussian09 package,[33] with the PBE density functional.[34] The standard 6-31G(d)[35,36] basis set was used for all H, C, N, F and O atoms; the Stuttgart triple zeta basis set (SDD),[37] along with the associated ECP to describe the 10 core electrons, was employed for Cu and Fe. In addition, an extra diffuse function[38] was employed in the optimization of negatively charged iron complexes. Solvation free energies are computed with the (IEF-PCM) continuum dielectric solvation model[39] using the radii and non-electrostatic terms by Truhlar and co-workers' SMD solvation model.[40] In all cases frequency calculations were carried out to ensure the nature of stationary points and transition states and to allow for the calculation of Gibbs free energies at 25 °C and 1 atm for all of the species involved in the catalytic cycles.

Additional single point calculations on the previously optimized geometries were carried out with a larger basis set. The 6-311+G** all-electron basis set[36] was used for all H, C, N, F and O atoms while the aug-cc-pVTZ-PP basis set including polarization and the associated electron core potential[41] was employed for Cu. In the case of Fe atoms, the all-electron aug-cc-pVTZ[42] basis set was used. The empirical dispersion terms were computed for the optimized geometries with the DFT-D3 package[43] by Grimme using the corresponding PBE-D[44] functional. Unless otherwise stated, all of the reported energy values correspond to the Gibbs free energies obtained with the large basis sets including solvation in acetone and the dispersion corrections.

As the mechanisms involve copper(I), copper(II) and copper(III) complexes with different multiplicities, different spin states are involved. Although we computed the triplet state in a number of cases, it was always found higher in

 

energy than the corresponding singlets, and because of that they are discussed in the text only in selected points.

Along the reaction pathways mononuclear and dinuclear species coexist, and it is not easy to assign a unique origin of energies for both species at the same time. In order to get a better numerical interpretation of the catalytic cycles a colour code is allocated to the computed free energy values; the black numbers correspond to the unique energy origin corresponding to a copper monomer, which means that the energies for the dimers are halved. In contrast, blue numbers correspond to energies calculated on the "dinuclear" scale, where two copper monomers are considered as the origin of energies. This colour coding is useful when trying to compare energy differences along the reaction pathways; thus, when comparing mononuclear and dinuclear species the black number is used whereas a comparison between two dinuclears is computed with the blue values.

## Results and discussion

### Outer sphere mechanisms for Glaser–Hay couplings

In this section, we describe the calculations used to explore the general mechanism for Glaser–Hay couplings where $K_3[Fe(CN)_6]$ is employed as the outer sphere oxidant.[6] Since there is no direct interaction between copper complexes and the oxidant, the latter is treated merely as the electron source in these mechanisms; the corresponding reduction half reaction is shown in eqn (1).

$$[Fe(CN)_6]^{3-} + 1e^- \rightarrow [Fe(CN)_6]^{4-} \quad (1)$$

First we describe the catalytic cycle for the phenylacetylene homocoupling reaction catalyzed by $[Cu(TMEDA)]^+$. Additional TMEDA units are used as bases, which are consistent with the excess of ligands usually introduced under Glaser–Hay conditions. A detailed description of this catalytic cycle is shown in Scheme 3 and all of the species along this pathway are named **GX** since they are related to this general catalytic cycle. In all of the schemes the copper atoms are colour-coded to indicate the oxidation state of the metal: copper(I) is black, copper(II) is red and copper(III) is purple; additionally, in most schemes the oxidation state of the copper atom is included between parenthesis. The catalytic cycle can be divided in three main steps: (i) alkyne deprotonation (from **G1** to **G3**), (ii) copper oxidation (from **G3** to **G5**), and (iii) reductive elimination (from **G5** to **G1**). The catalytic cycle starts with the π-coordination of phenylacetylene to the copper(I)–TMEDA complex (**G1**) to form the π-acetylene complex **G2**. This latter compound is more stable than the starting materials (−24.3 kcal $mol^{-1}$), and it seems plausible that the alkyne coordination to **G1** may be barrierless.

**G2** presents the expected trigonal geometry, with the metal coordinating both the $C_{sp}$ atoms. Next, the alkyne C–H terminal bond is activated by the base, a free TMEDA ligand, to yield the copper(I)-σ-acetylide complex (**G3**); this process is mediated by the corresponding transition state for deprotonation (**DP_TS**) which lies 17.5 kcal $mol^{-1}$ higher than **G2**. The alternative intramolecular deprotonation pathway, where TMEDA is bound to the metal before proton transfer, is also calculated, affording a very similar barrier (see ESI†). The relative energy of **G3** is around 4 kcal $mol^{-1}$ higher than that of **G2**, indicating that the deprotonation process is slightly endergonic. Detailed structures of **G2**, **DP_TS** and **G3** are provided in Fig. 1.

The dimerization of **G3** yields the corresponding copper(I) dinuclear species **G4**; in this intermediate both copper atoms adopt tetrahedral geometries, with the TMEDA ligands perpendicular to the $Cu_2$–$C_{(sp)2}$ planar core. This process is practically thermoneutral, as less than 1 kcal $mol^{-1}$ is required. The dicopper(I) complex **G4** is oxidized by the iron complexes to its dicopper(II) analog **G5**; just 4 kcal $mol^{-1}$ is required for this process. The **G5** complex corresponds to a closed-shell

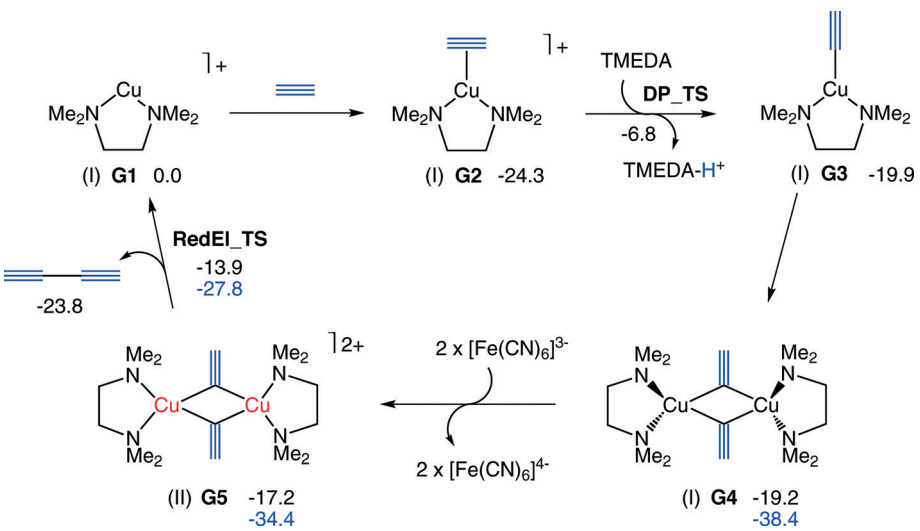


**Scheme 3** Proposed mechanism for Cu(I) Glaser–Hay coupling of phenylacetylene including the computed free energy values in kcal $mol^{-1}$ (phenylacetylene is depicted as ≡).

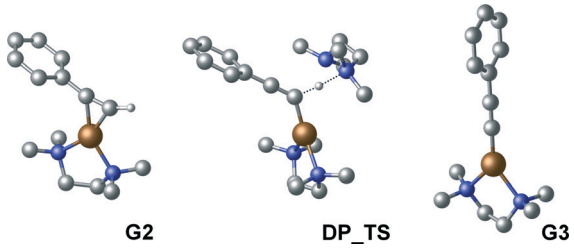


Fig. 1 Detailed structures of **G2**, **DP_TS** and **G3**.

singlet structure; with a bonding orbital delocalized in the two copper centers, the related triplet had a slightly higher energy. All of the attempts to locate the open-shell singlet analogue, with one unpaired electron on each copper(II) center *i.e.* the antiferromagnetic solution, were unsuccessful. Nevertheless it is expected that the energy difference between these three electronic states is small. **G5** is quite symmetrical: both copper atoms adopt almost square-planar geometries where the Cu–$C_{sp}$ distances are 1.96 and 1.99 Å. Interestingly, the $Cu_2C_2$ core is not planar; the angle between both copper planes is 127° and both acetylide substituents lie quite close ($C_{sp}$–$C_{sp}$ distance 2.49 Å). A detailed structural representation of intermediates **G4** and **G5** is found in Fig. 2. An alternative pathway associated to the alkynyl metathesis that would yield **G1** and a bisalkynyl copper(III) complex was studied and discarded because it was not possible to correctly optimize the latter structure.

The transition state for the bimetallic reductive elimination (**RedEl_TS**) is found to be only 6.6 kcal $mol^{-1}$ higher than **G5**, making this stage a very easy process. The geometry of this transition state, which looks very similar to **G5**, shows that the distance between the acetylide groups is shortened to 1.88 Å. The release of the coupled diphenyldiacetylene takes the catalytic cycle back to the starting point. The overall energetics indicate that the reaction is exergonic by 23.8 kcal $mol^{-1}$. The computed Gibbs free energies allow the calculation of the apparent activation energy for the reaction, which can be related to turnover frequency. This can be easily done by means of the energetic span model developed by Kozuch and Shaik.[45] This methodology states that the apparent activation barrier corresponds to the energy difference between the highest and the lowest species when the latter appears first in the catalytic cycle, as in our case of study. In this case the activation barrier is 17.5 kcal $mol^{-1}$ and corresponds to the deprotonation process of the coordinated alkyne (from **G2** to **DP_TS**). The magnitude of this barrier indicates that the reaction could be easily carried out at room temperature; moreover, the barrier is independent of the oxidant nature in agreement with the fact that any other oxidant stronger (or even slightly weaker) than $K_3[Fe(CN)_6]$ (+0.36 V) can be used to carry out this reaction. Our mechanism is also consistent with rate acceleration using stronger bases and more acidic alkynes, as both participate in the deprotonation step. This was further confirmed by the additional calculations summarized in Table 1.

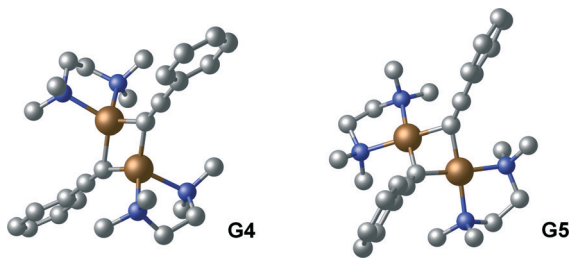


Fig. 2 Detailed structures of **G4** and **G5**.

In the computed catalytic cycle, all intermediates contain copper(I), except **G5** that has copper(II). **G5** is generated in the oxidation step and yields immediately a low barrier reductive elimination. Attempts to compute alternative catalytic cycles with an earlier oxidation step and more copper(II) intermediates produced higher energy barriers. The mechanism is nevertheless consistent with the experimental efficiency of systems where the catalyst is introduced as a copper(II) complex (*e.g.* $CuCl_2$, $Cu(OAc)_2$ or $Cu(NO_3)_2$ in the reaction media.[10,13] This requires a simple "precatalytic" cycle where copper(II) is converted into copper(I) by means of a preliminary alkyne homocoupling as described in the literature.[46] This precatalytic stage, depicted in Scheme 4, starts with the coordination of a free phenylacetylene to **G1′** to yield the π-acetylene complex **G2′**. Deprotonation, using a free TMEDA ligand, is an almost barrierless process since only 0.6 kcal $mol^{-1}$ are required. Once **G3′** is obtained the copper(II) dimer **G5** is formed, then reductive elimination takes place and the product is released, generating the copper(I) catalyst that may continue the catalytic reaction. The computed Gibbs free energies indicate that for this precatalytic stage the barrier is just 6.6 kcal $mol^{-1}$, corresponding to the bimetallic reductive elimination process (computed as the free energy difference between **G5** and **RedEl_TS**). Nevertheless, since the catalytic reaction corresponds to the one described in Scheme 3, the overall barrier for the whole reaction would be, as stated above, the alkyne deprotonation (17.5 kcal $mol^{-1}$). Scheme 4 shows a low energy pathway to reduce Cu(II) precursors to Cu(I) material to enter the catalytic cycle, though other mechanisms could also be envisaged involving participation of an external base or ligand metathesis. This is in any case a side question, as none of these steps participate in the main catalytic cycle.

Table 1 Rate limiting step dependence on the base and the substrate (kcal $mol^{-1}$)

| Base Influence | | | |
|---|---|---|---|
| Base | G2 | DP_TS | Barrier |
| $NH_3$ | −24.3 | −1.8 | 22.5 |
| TMEDA | −24.3 | −6.8 | 17.5 |
| $OH^-$ | −24.3 | −20.8 | 3.5 |
| **Substrate influence (R–PhC≡CH)** | | | |
| R | G2 | DP_TS | Barrier |
| *p*-F | −24.1 | −7.2 | 16.9 |
| *p*-H | −24.3 | −6.8 | 17.5 |
| *p*-Me | −25.7 | −7.3 | 18.4 |

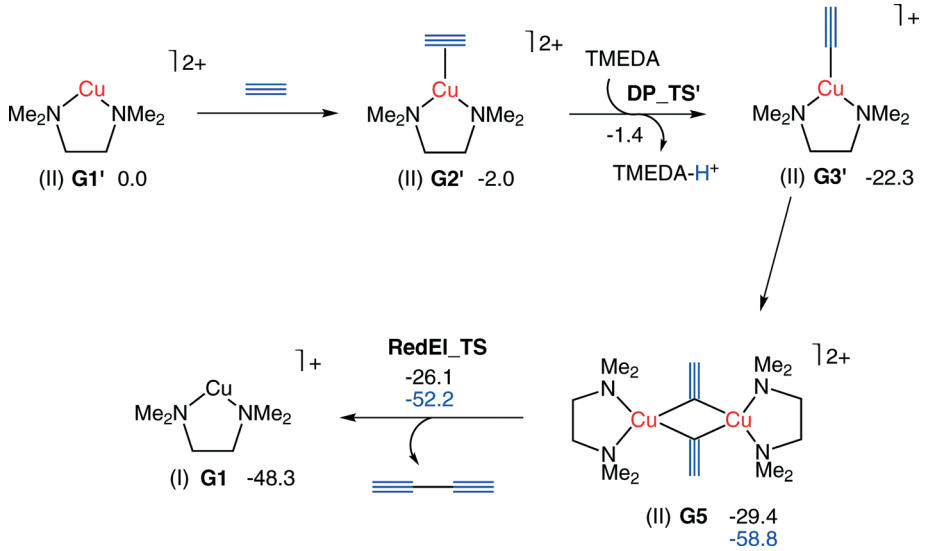


**Scheme 4** Proposed precatalytic cycle for the Cu(II)-catalyzed Glaser coupling of phenylacetylene including the computed free energy values in kcal mol$^{-1}$ (phenylacetylene is depicted as ≡).

A distinct alternative would be that the processes described in Scheme 4 comprise the main catalytic cycle, which could then be closed by the oxidation of **G1** to **G1′** by the external oxidant. This oxidation step would have a similar barrier to that of deprotonation in the main cycle reported above. However, we discarded this alternative mechanism, because in this case the rate would depend on the oxidant, and not on the nature of the base, in contrast to experimental observations.

### Inner sphere mechanism for the Glaser–Hay coupling: modeling the Cu–$O_2$ interactions

In this section the complete mechanism for the Glaser–Hay coupling using dioxygen as the oxidising agent is described. Although $O_2$ and some Cu/$O_2$ species are recognized as good outer sphere oxidants it should be expected that this kind of systems react following an inner sphere pathway;[27,28] in fact, the studied Cu(I)/TMEDA/$O_2$ system is reported to act as such in C–H activation processes.[47] The explicit use of dioxygen introduces a lot of additional steps in the catalytic cycle, and because of this we start by presenting a simplified picture of the overall mechanism in Scheme 5, where only the most significant species are shown. The three main steps described above (Scheme 3) for the reaction with the external oxidant are conserved: (i) alkyne deprotonation (from **G1** to **G3**), (ii) copper oxidation (from **G3** to **G5**), and (iii) reductive elimination (from **G5** to **G1**). Steps (i) and (iii) are identical, and will therefore not be further discussed. However, step (ii), the copper oxidation step, is much more complicated and can be divided in three additional substeps: (iia) dioxygen cleavage (from **G3** to **O5**), (iib) first oxygen protonation (from **O5** to **O13**), and (iic) second oxygen protonation and water extrusion (from **O13** to **G5**). In all cases species containing incoming oxygen atoms are noted as **OX** while species that have appeared before maintain the **GX** notation. All of the free energy values presented in these schemes and subsequent tables are computed using the same energy reference (**G1**).

Oxygen cleavage takes part in two steps (Scheme 6). Intermediate **G3**, resulting from alkyne deprotonation, reacts with $O_2$ (in the triplet state) and, after a 2-electron transfer, the σ-acetylide-copper(III)-η$^2$-peroxo complex **O4** is obtained. It was not possible to find any copper(I)-$O_2$ species, or copper(II)-superoxo complex, which may be formed prior to the electron transfer. The step from **G3** to **O4** involves a spin-crossing from triplet to singlet, likely through a low barrier minimum energy crossing point (MECP). In **O4** the copper atom adopts a slightly distorted square pyramidal structure, with the peroxo ion occupying two coordination sites and one nitrogen atom of the TMEDA ligand lying far in an axial position at 2.43 Å from the metal. The peroxide moiety is bound to copper in a side-on manner, with both Cu–O distances close to 1.89 Å. This first oxidation process is endergonic, as **O4** is 10.3 kcal mol$^{-1}$ higher than the previous intermediate. The coordination of a second **G3** complex to **O4** implies the second two-electron transfer and yields the bis(μ-oxo)-dicopper(III) complex **O5** (Fig. 3) which is only 3.9 kcal mol$^{-1}$ higher than **G3** (mononuclear energy scale). The relatively low free energy of **O5** is remarkable: there are several molecular units getting together to form this species, with the associated entropic penalty (see ESI†). This entropic penalty is compensated in this case by a substantial enthalphic gain. The structure of **O5** shows both copper atoms adopt square pyramidal geometries with one arm of the TMEDA ligand occupying the axial position at distances longer than 2.71 Å from the metal, based on the metal center electronic configuration (d$^8$). As expected, the $Cu_2O_2$ core is planar and almost symmetrical, with a Cu–Cu distance of 2.83 Å, the Cu–O distances are close to 1.84 Å and the O–O distance is 2.37 Å; in agreement with those measured experimentally for similar copper systems bearing nitrogen ligands.[28] This species

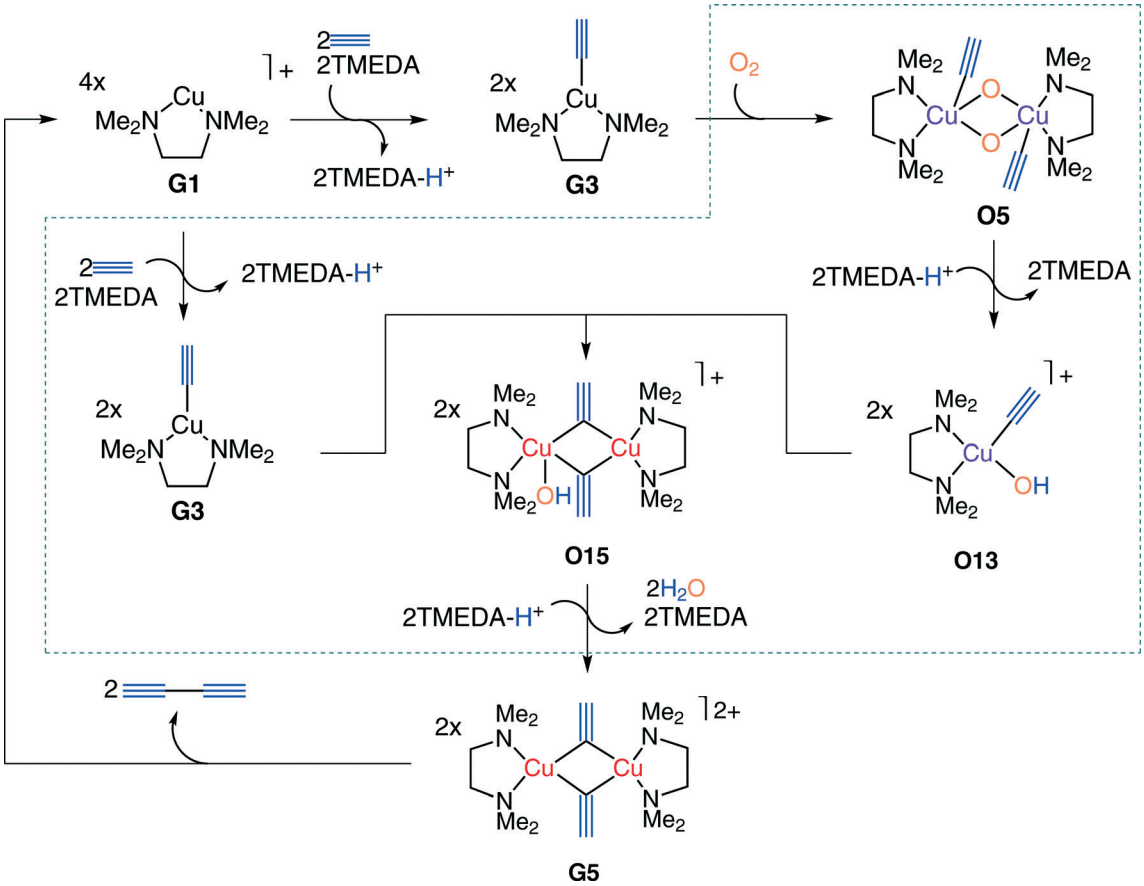


**Scheme 5** Simplified mechanism for the full catalytic cycle of the Glaser–Hay coupling of phenylacetylene using dioxygen as the oxidant (phenylacetylene is depicted as ≡). The dotted box highlights the intermediates involved in the oxidation step.

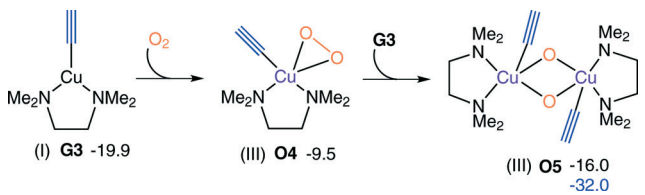


**Scheme 6** Proposed mechanism for oxygen cleavage in the Glaser–Hay coupling of phenylacetylene including the computed free energy values in kcal mol$^{-1}$ (phenylacetylene is depicted as ≡).

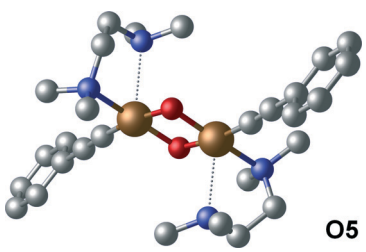


**Fig. 3** Detailed structure of **O5**.

is probably in equilibrium with its corresponding μ-η$^2$:η$^2$-peroxodicopper(II) complex; however, our calculations show that the latter lies more than 8 kcal mol$^{-1}$ higher than **O5**. We did not locate any transition states in the potential energy surface for these bimolecular processes, but if they exist, they should be fairly low. The highest energy of this oxygen cleavage step is that of **O4**, which at −9.5 kcal mol$^{-1}$ is well below the energy of the preceding transition step for alkyne deprotonation. After oxygen cleavage comes substep (iib), the first proton transfer to oxygen. The best pathway we have found for this process is shown in Scheme 7 where the TMEDA ligands act as proton shuttles that allow the cleavage of the $Cu_2O_2$ core. Of course, alternative pathways are plausible (see ESI†) and it would not be unexpected that the reaction could proceed by one of those to give rise to the same product formation with energy requirements not very different to the ones shown here. In the pathway proposed in Scheme 7, the reaction proceeds from **O5** by the cleavage of the C–$N_{axial}$ bond in one of the copper atoms; a step that requires less than 2 kcal mol$^{-1}$. Once **O6** is formed, a proton transfer between nitrogen and one of the free protonated TMEDA ligands (obtained in the acetylene deprotonation step) occurs. This process, which is endergonic by another 7.2 kcal mol$^{-1}$, yields the complex **O7**. Then a proton transfer occurs between TMEDA and the oxygen atom and **O9**, with protonated bridge oxygen, is obtained. The second bridge protonation follows the same reaction sequence until complex **O12**, with the two bridging oxygen atoms protonated. After the proton transfer to the oxygen atom the dimeric

 

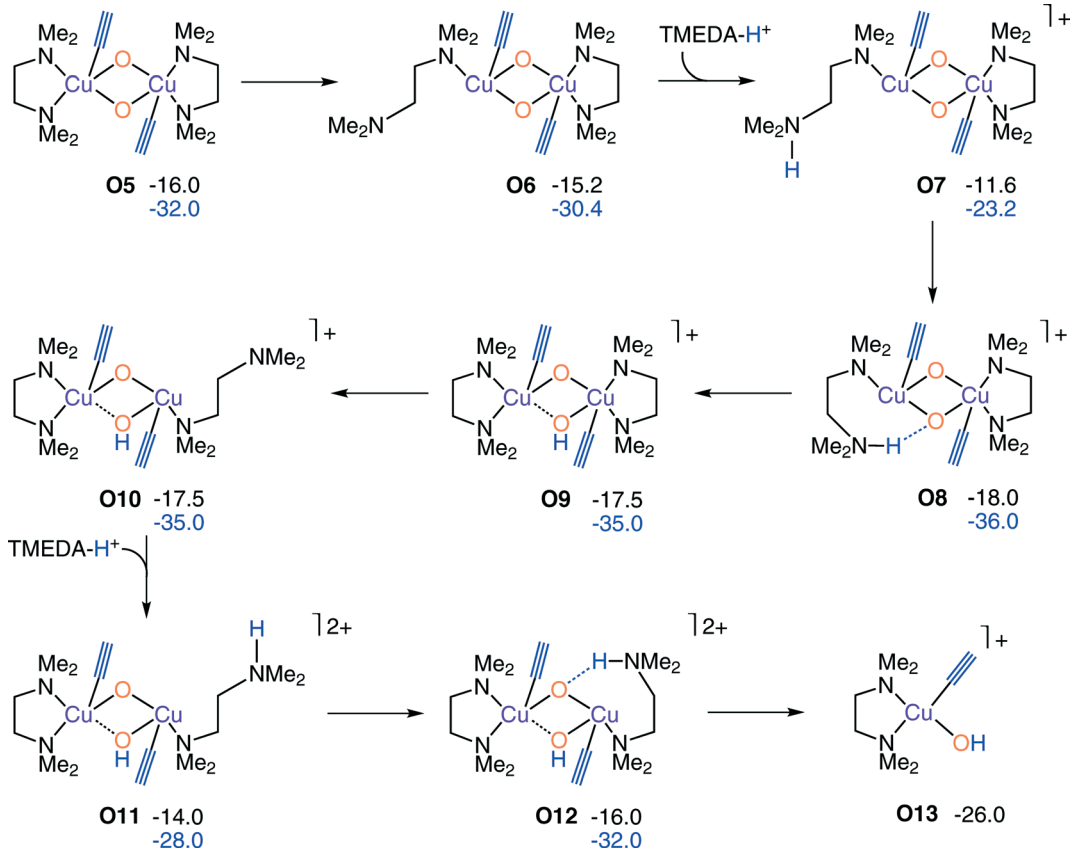


**Scheme 7** Proposed mechanism for bis-oxo bridge protonation in the Glaser–Hay coupling of phenylacetylene including the computed free energy values in kcal mol$^{-1}$ (phenylacetylene is depicted as ≡).

species are no longer stable and two monomeric **O13** species are formed; this copper(III) intermediate adopts the expected square planar geometry and constitutes the lowest free energy point in the catalytic cycle so far. Process (iib) involves minor energy changes in most steps and does not change the identity of the previously determined rate-limiting steps. The metal remains as copper(III) through all of these steps.

The reaction follows then the pathway shown in Scheme 8 where a water molecule is removed from the system. **O13** reacts with the copper(I) intermediate **G3** formed during the first steps of the reaction; the formation of the dimeric species **O14** involves a concomitant one-electron transfer from one copper center to the other one through the bridging alkynyl and hydroxyl groups. At this point, our mechanistic proposal diverges from that of Fomina and coworkers, as they proposed the formation of dimeric species from the equivalent of two **O13** units.[23] This complex would be a copper(III) dimer, and has a completely different behaviour and a substantially higher energy than the copper(II) dimer we are proposing. The conversion from **O13** plus **G3** to **O14** is almost thermoneutral (only 1.5 kcal mol$^{-1}$ are required) and yields a structure where the bridging groups lie practically at the same distance from both copper atoms. A small rearrangement of ligands in **O14**, where the hydroxo bridging group is replaced by the second alkyne, provides the bis-μ-alkynyl dimer **O15**.

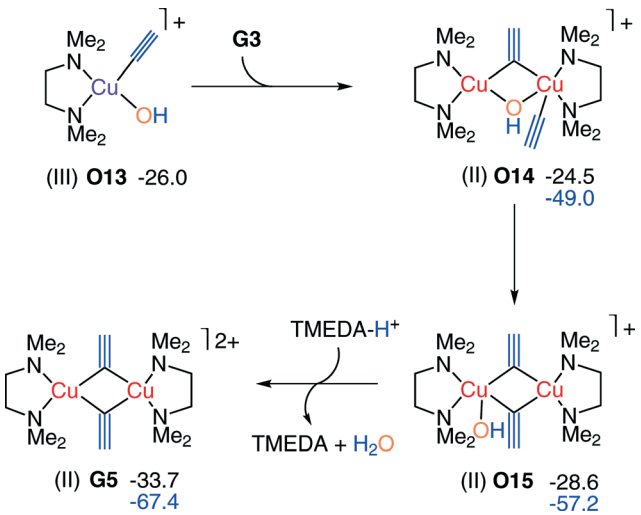


**Scheme 8** Proposed mechanism for the second oxygen protonation and water extrusion in the Glaser–Hay coupling of phenylacetylene including the computed free energy values in kcal mol$^{-1}$ (phenylacetylene is depicted as ≡).

The protonation of the hydroxyl group by TMEDA-H$^+$ produces one molecule of water and the dinuclear species **G5** that is ready for the reductive elimination step described above in the outer-sphere mechanism. This second

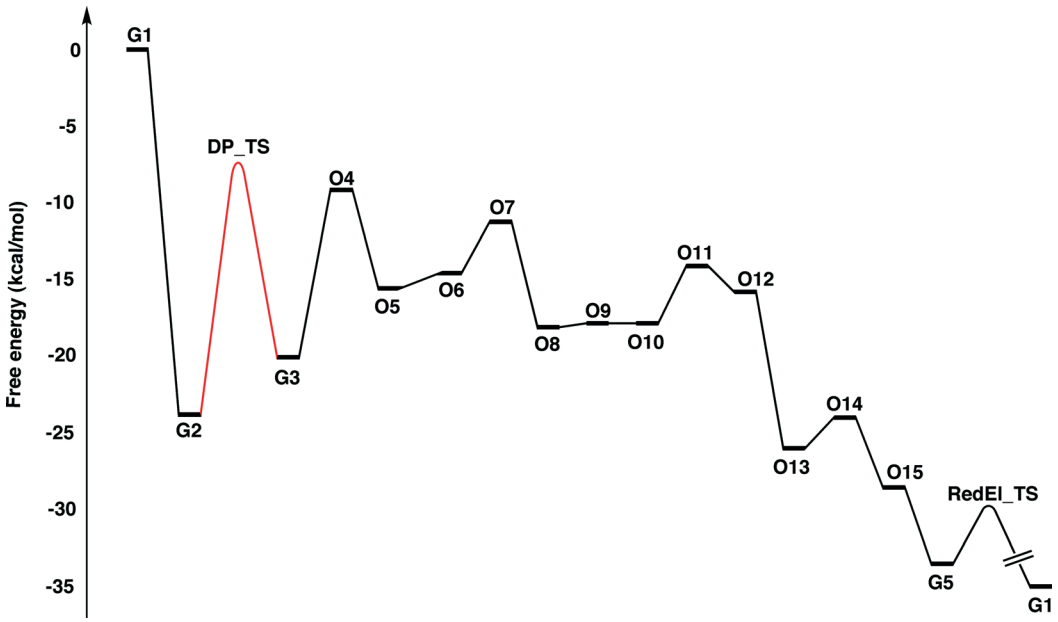


**Scheme 9** Complete free energy profile (in kcal $mol^{-1}$) for the Glaser–Hay reaction. The rate-limiting step is indicated in red.

protonation and extrusion process is a downhill sequence that does not bring any significant barrier to the overall catalytic cycle.

The reaction energy, computed as the formation of a diphenyldiacetylene from two phenylacetylenes and one half of dioxygen, is exergonic by 56.9 kcal $mol^{-1}$, in agreement with the strong oxidizing power of $O_2$ to $H_2O$. Although the mechanism for this inner sphere oxidant looks more complicated than the one for outer sphere oxidants, the apparent reaction barrier[45] remains the same (17.5 kcal $mol^{-1}$) corresponding to the deprotonation of the coordinated alkyne, confirming that the reaction rate is independent of the nature of the oxidant and indicating that it should work smoothly at room temperature. Scheme 9 shows the complete free energy profile of the studied reaction, with the key step from **G2** to **DP_TS** highlighted. It is also worth mentioning that copper(III) intermediates appear when dioxygen is used, pointing to a more specific role for copper in this particular case.

Of course, it would be possible to think about an outer sphere mechanism involving dioxygen, where a $\eta^1$-superoxocopper(II) or a $\eta^2$-peroxocopper(III) could act as an oxidant. This alternative pathway is also computed and can be found in the ESI.† The barriers found are quite low, but still higher than those of the inner sphere mechanism described here. Moreover, an outer sphere mechanism would not comply with what is observed experimentally for similar systems *i.e.* whenever TMEDA is used along copper in the presence of dioxygen the dinuclear bis(μ-oxo)-dicopper(III) complexes are observed.[47] These results favoring the inner sphere may seem to be in contrast to the fact that most experimental evidence on copper–dioxygen interactions focuses on the intermediates of outer sphere electron transfers.[26–28] A more careful analysis of the experimental literature shows however that the observation of these intermediates requires the use of specific, usually bulky ligands in the understanding that in the absence of those an inner sphere mechanism would operate.[27]

## Conclusions

The mechanism for the Glaser–Hay oxidative coupling of terminal alkynes is characterized by DFT calculations. In the case of copper(I) coupling where an outer sphere oxidant is employed, the mechanism resembles the classical Bohlmann proposal: first the alkyne coordinates to copper, enhancing the acidity of the terminal proton that can be abstracted by an external base. After deprotonation copper(I)-σ-acetylide dimerizes and can be oxidized by most outer-sphere oxidants to yield the corresponding copper(II) dimers; finally, a fast bimetallic reductive elimination yields the product. When copper(II) is used as starting material, there is a minor nuance in the form of a low barrier precatalytic cycle where the first 1,3-diyne unit is produced, the mechanism then reverts to that for copper(I) catalysts.

In the case where dioxygen is employed as the inner-sphere oxidant, the mechanism follows a pathway similar to that of natural oxidases. Bis(μ-oxo)-dicopper(III) complexes are formed in the first instance, and after protonation of the bridge the reaction between copper(I) and copper(III) yields the same copper(II) dimers as in the outer-sphere mechanism and, from those, the $C_{sp}$–$C_{sp}$ coupling reaction is quite easy.

The rate-limiting step for all of the studied reactions corresponds to the Cu-coordinated alkyne deprotonation, demonstrating why more acidic acetylenes and stronger bases provide higher reaction rates. In addition, the calculated barrier is low enough (17.5 kcal $mol^{-1}$) to allow the reaction to proceed at room temperature, as observed experimentally.

## Notes and references


1 R. Bates, *Organic Synthesis using Transition Metals*, Wiley-Blackwell, Sheffield, UK, 2000; J. F. Hartwig, *Organotransition Metal Chemistry: From Bonding to Catalysis*, University Science Books, U.S., Sausalito, US, 2009.

2 The Nobel Prize in Chemistry 2010 – Richard F. Heck and E.-I. Negishi, Akira Suzuki Nobelprize.org. 6 June 2010. http://nobelprize.org/nobel_prizes/chemistry/laureates/2010/.

3 T. Hamada, X. Ye and S. S. Stahl, *J. Am. Chem. Soc.*, 2008, **130**, 833; W. Yin, C. He, M. Chen, H. Zhang and A. Lei, *Org. Lett.*, 2008, **11**, 709; X. Guo, R. Yu, H. Li and Z. Li, *J. Am. Chem. Soc.*, 2009, **131**, 17387; R. J. Lundgren and M. Stradiotto, *Angew. Chem., Int. Ed.*, 2010, **49**, 9322.

4 P. Tundo, P. Anastas, D. S. Black, J. Breen, T. Collins, S. Memoli, J. Miyamoto, M. Poliakoff and W. Tumas, *Pure Appl. Chem.*, 2000, **72**, 12007.

5 C. Glaser, *Ber. Dtsch. Chem. Ges.*, 1869, **2**, 422; C. Glaser, *Justus Liebigs Ann. Chem.*, 1870, **154**, 137.

6 A. Baeyer and L. Landsberg, *Ber. Dtsch. Chem. Ges.*, 1882, **15**, 57; F. J. Brockman, *Can. J. Chem.*, 1955, **33**, 507.

7 A. Vaitiekuans and F. F. Nord, *J. Am. Chem. Soc.*, 1954, **76**, 2733; Y. Odaira, *Bull. Chem. Soc. Jpn.*, 1956, **29**, 470; P. Siemsen, R. C. Livingston and F. Diederich, *Angew. Chem., Int. Ed.*, 2000, **39**, 2632; J. J. Li, *Name Reactions for Homologation, Part 1*, John Wiley & Sons Inc., Hoboken, New Jersey, 2009.

8 A. Hay, *J. Org. Chem.*, 1960, **25**, 1275; A. S. Hay, *J. Org. Chem.*, 1962, **27**, 3320.

9 E. Valentí, M. A. Pericàs and F. Serratosa, *J. Am. Chem. Soc.*, 1990, **112**, 7405; N. Hebert, A. Beck, R. B. Lennox and G. Just, *J. Org. Chem.*, 1992, **57**, 1777; E. W. Kwock, T. Baird and T. M. Miller, *Macromolecules*, 1993, **26**, 2935; F. M. Menger, X. Y. Chen, S. Brocchini, H. P. Hopkins and D. Hamilton, *J. Am. Chem. Soc.*, 1993, **115**, 6600; D. W. J. McCallien and J. K. M. Sanders, *J. Am. Chem. Soc.*, 1995, **117**, 6611; S. Hoger, A.-D. Meckenstock and H. Pellen, *J. Org. Chem.*, 1997, **62**, 4556; R. E. Martin, T. Mäder and F. Diederich, *Angew. Chem., Int. Ed.*, 1999, **38**, 817; M. A. Heuft, S. K. Collins, G. P. A. Yap and A. G. Fallis, *Org. Lett.*, 2001, **3**, 2883; K. Miyawaki, R. Goto, T. Takagi and M. Shibakami, *Synlett*, 2002, 1467; X. Xie, P.-W. Phuan and M. C. Kozlowski, *Angew. Chem., Int. Ed.*, 2003, **42**, 2168; Q. Zheng and J. A. Gladysz, *J. Am. Chem. Soc.*, 2005, **127**, 10508; L. Chu and F.-L. Qing, *J. Am. Chem. Soc.*, 2010, **132**, 7262; X. Jia, K. Yin, C. Li, J. Li and H. Bian, *Green Chem.*, 2011, **13**, 2175; K. Yin, C. Li, J. Li and X. Jia, *Green Chem.*, 2011, **13**, 591; S. Zhang, X. Liu and T. Wang, *Adv. Synth. Catal.*, 2011, **353**, 1463; S. E. Allen, R. R. Walvoord, R. Padilla-Salinas and M. C. Kozlowski, *Chem. Rev.*, 2013, **113**, 6234.

10 J. J. Pak, T. J. R. Weakley and M. M. Haley, *J. Am. Chem. Soc.*, 1999, **121**, 8182.

11 L. Li, J. Wang, G. Zhang and Q. Liu, *Tetrahedron Lett.*, 2009, **50**, 4033.

12 Q. Zheng, R. Hua and Y. Wan, *Appl. Organomet. Chem.*, 2010, **24**, 314.

13 H. A. Stefani, A. S. Guarezemini and R. Cella, *Tetrahedron*, 2010, **66**, 7871.

14 D. Li, K. Yin, J. Li and X. Jia, *Tetrahedron Lett.*, 2008, **49**, 5918.

15 K. Yin, C.-J. Li, J. Li and X.-S. Jia, *Appl. Organomet. Chem.*, 2011, **25**, 16.

16 F. Bohlmann, H. Schönowsky, E. Inhoffen and G. Grau, *Chem. Ber.*, 1964, **97**, 794.

17 M. B. Nielsen and F. Diederich, *Chem. Rev.*, 2005, **105**, 1837.

18 A. Stütz, *Angew. Chem., Int. Ed. Engl.*, 1987, **26**, 320.

19 P. J. Stang and F. Diederich, *Modern Acetylene Chemistry*, Weinheim, 1995; J. M. Tour, *Chem. Rev.*, 1996, **96**, 537.

20 A. E. Wendlandt, A. M. Suess and S. S. Stahl, *Angew. Chem., Int. Ed.*, 2011, **50**, 11062; A. N. Campbell and S. S. Stahl, *Acc. Chem. Res.*, 2012, **45**, 851.

21 Q. Liu, P. Wu, Y. Yang, Z. Zeng, J. Liu, H. Yi and A. Lei, *Angew. Chem., Int. Ed.*, 2012, **51**, 4666; Y.-F. Wang, H. Chen, X. Zhu and S. Chiba, *J. Am. Chem. Soc.*, 2012, **134**, 11980.

22 C. Sens, I. Romero, M. Rodríguez, A. Llobet, T. Parella and J. Benet-Buchholz, *J. Am. Chem. Soc.*, 2004, **126**, 7798; L. Duan, F. Bozoglian, S. Mandal, B. Stewart, T. Privalov, A. Llobet and L. Sun, *Nat. Chem.*, 2012, **4**, 418; M. L. Rigsby, S. Mandal, W. Nam, L. C. Spencer, A. Llobet and S. S. Stahl, *Chem. Sci.*, 2012, **3**, 3058.

23 L. Fomina, B. Vazquez, E. Tkatchouk and S. Fomine, *Tetrahedron*, 2002, **58**, 6741.

24 C. J. Cramer, A. Kinal, M. Włoch, P. Piecuch and L. Gagliardi, *J. Phys. Chem. A*, 2006, **110**, 11557; C. J. Cramer, M. Włoch, P. Piecuch, C. Puzzarini and L. Gagliardi, *J. Phys. Chem. A*, 2006, **110**, 1991.

25 B. F. Gherman and C. J. Cramer, *Coord. Chem. Rev.*, 2009, **253**, 723.

26 A. P. Cole, D. E. Root, P. Mukherjee, E. I. Solomon and T. D. P. Stack, *Science*, 1996, **273**, 1848; E. I. Solomon, U. M. Sundaram and T. E. Machonkin, *Chem. Rev.*, 1996, **96**, 2563; L. Q. Hatcher and K. D. Karlin, *JBIC, J. Biol. Inorg. Chem.*, 2004, **9**, 669.

27 E. A. Lewis and W. B. Tolman, *Chem. Rev.*, 2004, **104**, 1047.

28 L. M. Mirica, X. Ottenwaelder and T. D. P. Stack, *Chem. Rev.*, 2004, **104**, 1013.

29 P. Kang, E. Bobyr, J. Dustman, K. O. Hodgson, B. Hedman, E. I. Solomon and T. D. P. Stack, *Inorg. Chem.*, 2010, **49**, 11030; Y. Gao, G. Wang, L. Chen, P. Xu, Y. Zhao, Y. Zhou and L.-B. Han, *J. Am. Chem. Soc.*, 2009, **131**, 7956; H. Rao, H. Fu, Y. Jiang and Y. Zhao, *Adv. Synth. Catal.*, 2010, **352**, 458; J.-S. Tian and T.-P. Loh, *Angew. Chem., Int. Ed.*, 2010, **49**, 8417; Y. Wei, H. Zhao, J. Kan, W. Su and M. Hong, *J. Am. Chem. Soc.*, 2010, **132**, 2522; C. Zhang and N. Jiao, *Angew. Chem., Int. Ed.*, 2010, **49**, 6174.

30 N. Hewitt and A. Rauk, *J. Phys. Chem. B*, 2009, **113**, 1202; J. Jover and F. Maseras, *Chem. Commun.*, 2013, **49**, 10486.

31 M. García-Melchor, A. A. C. Braga, A. Lledós, G. Ujaque and F. Maseras, *Acc. Chem. Res.*, 2013, **46**, 2626; A. A. C. Braga, N. H. Morgon, G. Ujaque and F. Maseras, *J. Am. Chem. Soc.*, 2005, **127**, 9298; A. Nova, G. Ujaque, F. Maseras, A. Lledós and P. Espinet, *J. Am. Chem. Soc.*, 2006, **128**, 14571; B. Fuentes, M. García-Melchor, A. Lledós, F. Maseras, J. A. Casares, G. Ujaque and P. Espinet, *Chem. – Eur. J.*, 2010,

**16**, 8596; C. Mollar, M. Besora, F. Maseras, G. Asensio and M. Medio-Simón, *Chem. – Eur. J.*, 2010, **16**, 13390.

32 G. J. Christian, A. Llobet and F. Maseras, *Inorg. Chem.*, 2010, **49**, 5977; A. Conde, L. Vilella, D. Balcells, M. M. Díaz-Requejo, A. Lledós and P. J. Pérez, *J. Am. Chem. Soc.*, 2013, **135**, 3887.

33 M. J. Frisch, G. W. Trucks, H. B. Schlegel, G. E. Scuseria, M. A. Robb, J. R. Cheeseman, G. Scalmani, V. Barone, B. Mennucci, G. A. Petersson, H. Nakatsuji, M. Caricato, X. Li, H. P. Hratchian, A. F. Izmaylov, J. Bloino, G. Zheng, J. L. Sonnenberg, M. Hada, M. Ehara, K. Toyota, R. Fukuda, J. Hasegawa, M. Ishida, T. Nakajima, Y. Honda, O. Kitao, H. Nakai, T. Vreven, J. A. Montgomery, Jr, J. E. Peralta, F. Ogliaro, M. Bearpark, J. J. Heyd, E. Brothers, K. N. Kudin, V. N. Staroverov, R. Kobayashi, J. Normand, K. Raghavachari, A. Rendell, J. C. Burant, S. S. Iyengar, J. Tomasi, M. Cossi, N. Rega, N. J. Millam, M. Klene, J. E. Knox, J. B. Cross, V. Bakken, C. Adamo, J. Jaramillo, R. Gomperts, R. E. Stratmann, O. Yazyev, A. J. Austin, R. Cammi, C. Pomelli, J. W. Ochterski, R. L. Martin, K. Morokuma, V. G. Zakrzewski, G. A. Voth, P. Salvador, J. J. Dannenberg, S. Dapprich, A. D. Daniels, Ö. Farkas, J. B. Foresman, J. V. Ortiz, J. Cioslowski and D. J. Fox, *Gaussian09, Revision A.02*, (2009), Gaussian, Inc., Wallingford CT.

34 J. P. Perdew, K. Burke and M. Ernzerhof, *Phys. Rev. Lett.*, 1996, 77, 3865; J. P. Perdew, K. Burke and M. Ernzerhof, *Phys. Rev. Lett.*, 1997, **78**, 1396.

35 P. C. Hariharan and J. A. Pople, *Theor. Chim. Acta*, 1973, **28**, 213.

36 M. J. Frisch, J. A. Pople and J. S. Binkley, *J. Chem. Phys.*, 1984, **80**, 3265.

37 T. H. Dunning and P. J. Hay, in *Modern Theoretical Chemistry*, ed. H. F. Schaefer III, Plenum, New York, 1976, vol. 3, p. 1; A. Bergner, M. Dolg, W. Küchle, H. Stoll and H. Preuss, *Mol. Phys.*, 1993, **80**, 1431.

38 T. Clark, J. Chandrasekhar, G. W. Spitznagel and P. V. R. Schleyer, *J. Comput. Chem.*, 1983, **4**, 294.

39 D. J. Tannor, B. Marten, R. Murphy, R. A. Friesner, D. Sitkoff, A. Nicholls, B. Honig, M. Ringnalda and W. A. Goddard, *J. Am. Chem. Soc.*, 1994, **116**, 11875; B. Marten, K. Kim, C. Cortis, R. A. Friesner, R. B. Murphy, M. N. Ringnalda, D. Sitkoff and B. Honig, *J. Phys. Chem.*, 1996, **100**, 11775.

40 A. V. Marenich, C. J. Cramer and D. G. Truhlar, *J. Phys. Chem. B*, 2009, **113**, 6378.

41 K. A. Peterson and C. Puzzarini, *Theor. Chem. Acc.*, 2005, **114**, 283.

42 N. B. Balabanov and K. A. Peterson, *J. Chem. Phys.*, 2005, **123**, 064107.

43 *DFT-D3 A dispersion correction for density functionals, Hartree-Fock and semi-empirical quantum chemical methods*, Universität Bonn, 2011.

44 S. Grimme, *J. Comput. Chem.*, 2004, **25**, 1463; S. Grimme, *J. Comput. Chem.*, 2006, **27**, 1787; S. Grimme, *J. Chem. Phys.*, 2010, **132**, 154104.

45 S. Kozuch and S. Shaik, *Acc. Chem. Res.*, 2010, **44**, 101.

46 W. S. Brotherton, H. A. Michaels, J. T. Simmons, R. J. Clark, N. S. Dalal and L. Zhu, *Org. Lett.*, 2009, **11**, 4954; G. Zhang, H. Yi, G. Zhang, Y. Deng, R. Bai, H. Zhang, J. T. Miller, A. J. Kropf, E. E. Bunel and A. Lei, *J. Am. Chem. Soc.*, 2014, **136**, 924.

47 P. Kang, E. Bobyr, J. Dustman, K. O. Hodgson, B. Hedman, E. I. Solomon and T. D. P. Stack, *Inorg. Chem.*, 2010, **49**, 11030.

 